Contents

3. Charging Characteristics of Materials: Comparison of Experimental Results with Simple Analytical Models

Carolyn K. Purvis, N. John Stevens, and Jon C. Oglebay
Lewis Research Center
Cleveland, Ohio

Abstract

An understanding of the behavior of materials, of dielectrics in partitular, under charged particle bombardment is essential tb the prediction and prevention of the adverse effects of spacecraft charging. This paper presents an effort to Obtain Buch an understanding through a combined analytital and experimental approach.

A one-dimensional model for charging of samples in the LeRC test facility is used in conjunction with experimental data taken in this facility to develbp "material charging characteristics" for silvered Teflon. These characteristics are then used in a one dimensional model for charging in space to examine expected response. Relative Charging Pates as well as relative charging levels for silvered Teflon and metal ate discussed.

1. INTRODUCTION

Two previous papers[1,2] described the test facility, test methods and measurementis, arid the results bf various materials characteristics test performed at the Lewis Research Center in support of the spacecraft charging investigation. The

present paper summarizes the analytical work which has been performed interactively wtth this experimental work, The goal of the analysis is twofold. Firbt, is tb model the charging of material samples in terms of the material's parameters. Second, since a goal of the entire study is to predict behavior of spacecraft surfaces, an attempt is made to "scale" the environment, that is, to relate results obtained using a monoenergetic beam in the ground teat facility to expected results with distributed particle fluxes of the space environment. An approach tb establish this environment scaling is tb develop models of charging fbr both charged particle environments, and assume that the material properties are constant. "hen differences between material charging behavior under grbund teat end in space are a result of the differences in the two environments. It is recognized that the vacuum levels in the ground test and space environments are also different. Nu attempt is made here to account for this factbr.

This paper, then, represent, a first attempt at attaining the two goals of characterizing material charging and scaling to the space environment. The models used are one-dimensional and describe charging of Bamples in terms of the charging of a capacitor. This type of model has been used by a number of workers[3,4,5,6] to describe Spacecraft charging.

The procedure used herein was to first develop a one-dimensional model tb describe charging of samples in the LeRC vacuum test facility. This model codtained a number of parameters which were varied to provide best fits to experimental data obtained in the facility. The values of these parameters which yielded the belt fit were identified as the "material charging characteristics." These were then used in conjunction with a one-dimensional model for chargidg id the space substorm environment to make some predictions of the charging behavior of the materials in space. The insulatbr studied here is 5 mil silvered FEP® Teflon.

2. ONE-DIMENSIONAL (1-D) GROUND TEST FACILITY MODEL

In the LeRC test facility, a monoenergetic beam of electrons with energies of ~2 to 20 keV is directed at normal incidence to planar samples. A beam current density of 1 nA/cm^2 wad used to obtain all teat data discussed in this report.

The Ground Test Facility Model is a quasistatic current balance model. The current densities considered are those due to primary (beam) electrons, secondary electrons, backscattered electrbns, and leakage current through the sample bulk. These are denoted by j_e, j_s, j_{BS}, and j_l, respectively. The sample is assumed to charge like a capacitor. Thus a time balance equation is of the form

$$C \frac{dV_s}{dt} + j_l = j_e - j_s - j_{BS} \qquad (1)$$

where V_s is the magnitude of the surface voltage. All signs are explicit in this equation, and in all others used in the test facility model, that is, all symbols stand for positive numbers. The actual surface voltage is of course negative, and this is assumed throughout. Thus thts model does nbt predict positive surface voltages correctly, since positive surface voltage would tend to reattract the emitted secondary electrons add this effect has not been included here.

The first term in Eq. (1) represents the net sharp deposited od the surface (per cm^2) in a tin e step, add so is termed the! charging current deneity and denoted by j_c. The procedure ubed was to initialize at t = 0 with V_s = I). Then ΔV_s was calculated from

$$\frac{\Delta V_s}{\Delta t} = \frac{1}{C}\left[j_e - j_s - j_{BS} - j_l\right] . \qquad (2)$$

The current densities are all functions of V_s and their functional forms are giveh in Figure 1. Equation (2) is solved by an iterative procedure. This equation can be expressed as

$$\nabla V_s = f(V_s)\,\Delta t \quad . \qquad (3)$$

With the initial assumption V_s = t = 0, a suitable At is choseh, atld ΔV_s calculated, V_s is then incremented by ΔV_s (set = ΔV_s fbr the first iteration) arid the procedure repeated until equilibrium is reached, that is, until

$$j_c = C\frac{dV_s}{dt} = 0$$

The several current densities in the preceding equations are functions of surface voltage. All but the leakage curtent density are functions of the primary electron beam voltage and current density. The parameters whieh can be varied are the secondary emission maximum yield, δ_m, and energy for maximum yield, V_m the backscatter coefficient, η, the resistivity, ρ, and the capacitance! C. In practice, values for δ_m and V_m were taken from the literature. Values for ρ were determined from the measured surface voltages and currents at equilibrium, and fits obtained by varying fand C. This is discussed more fully in Section 4.

It should be noted that this madel does not account for beam spread in angle or energy, the presence of the vacuum tank wails, or residual gas in the; chamber. Since it is one-dimenstonal, it can not, of course, explicitly describe edge effects, or effects due to surface variations.

Derivations of the current density equations are presented in Appendtx A. A summary of the madel and equations is given in Figure 1.

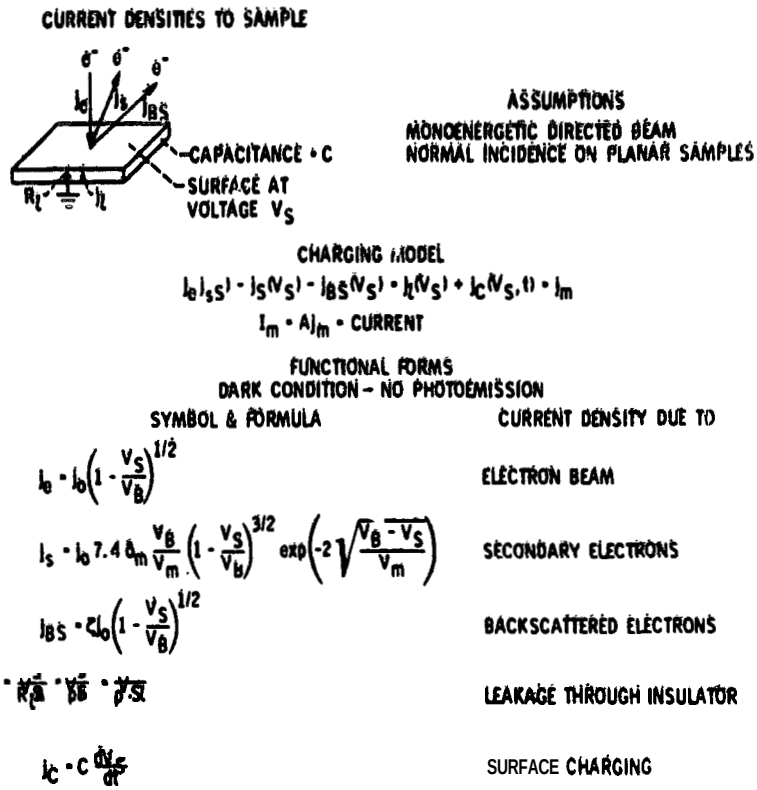

Figure 1. 1-D Model Ground Test Environment

3. COMPARISON WITH EXPERIMENTAL DATA

3.1 "Floating" Aluminum Plate

The first test data used in conjunction with the test facility charging model were those taken with a bare aluminum plate which is normally used for substrates. This plate Was mounted in front of a second identical plate which was grounded to the chamber walls. These two plates were held apart and electrically isolated by a Teflon spacer plug 0.7 cm long. The plates ate rectangular with dimensibns 15 cm X 20 cm (~300 cm^2 area). Surface voltage of the floating plate was measured as a function of time using the surface voltage probe. 1

Figure 2 shows these data and the best fit calculated curves. In obtaining these fits to the data, values of $\delta_m = 3$ and $V_{max} = 400$ were used. These are consistent with ranges of values for these parameters given by Gibbons[7] for a surface layer of Al_2O_3. It is reaeonable to expect some oxide on the surface of the "bare aluminum" plate since It had in fact been exposed to air. This points up

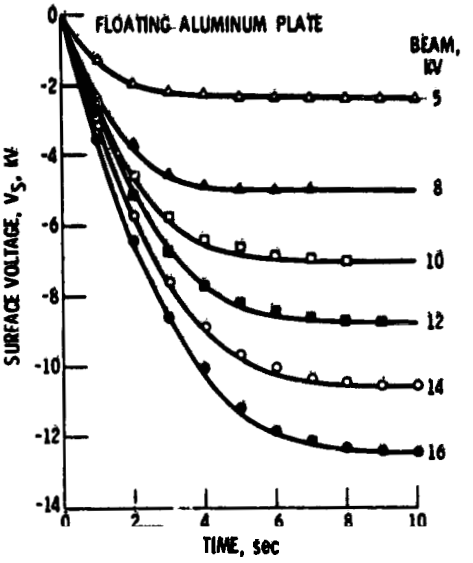

Figure 2. Comparison With Experimetital Data

the strong dependence of charging phenomena on sample surface cohdition, and indicates that care must be taken in making predictions for charging ti, consider the state of the surface.

With these values in the expression for secondary emission, the values of C used to obtain the curves in Figure 2 Varied from 1.2×10^{-10} farads at V_B = 5kV to 5×10^{-11} farads at V_B = 16 kV, decreasing approximately linearly with increasing beam voltage. The values used for the "backscatter coefficient" varied from 0. 15 at V_B = 5 kV to 0. 5 at V_B = 16 kV, again in approximately linear fashion. The expression used to calculate secondary emission current density is derivkd from an expression for yield as a function bf primary energy due to Sternglass.[8] It is plausible that the required variation of ξ to obtain fits to the data is accounted for, in part, by deviations of the actual secondary yield from that predicted by Sternglass formula. That is, the adjustments to ξ represeht adjustments to the sum of the backscattered and secondary electrons.

The final point of concern here is the time scale for charging of the floating plate; it Peaches its equilibrium floating vdltage With a time constant of several seconds. This is not surprising, since the capacitance of the test plate to its surroundings is expected to be small. The timescale, is relevant, However. to the question of the behavior of composite samples. This is discussed more fully in Section 3. 3.

3.2 Silvered Teflon Samples

The 1-b model Was next used t6 fit current and sutface voltage data from silvered Teflon samples. These consist of an aluminum substrate with three strips of 5 mtl silvered Teflon mounted with conductive adhesive to the substrate. Each of these strips was 5 cm wide and 20 cm long. During test, the aluminum substrate (and consequently the silver) wad grounded, while the Teflon surface was bombarddd with electrons.

The data and calculated fits for beam voltages at which equilibrium is reached; are shown in Figure 3. These data are a composite of four separate data sets, and indicate charging times on the order of minutes. The error bat's reflect the scatter in the data as well as the f5 percent resolution uncertainty in the voltage measurements. Since for insulators there are strong voltage gradients near the edges of the sample#, the Surface voltage measurements ate those read at the sample center Which is uniform.

To obtain these curves, the effective resistance was calculated from the equilibrium values of surface voltage and leakage current. These values indicate an effective resistivity for the samples of about 9×10^{15} Ω-cm, about an order of

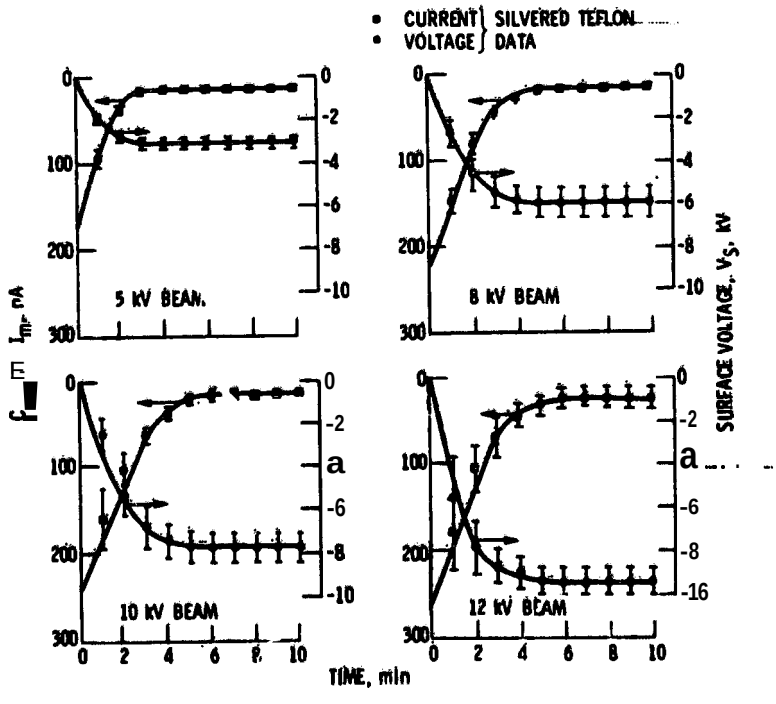

Figure 3. Comparison Wlth Experimental Data. 5 Mtl Silvered Teflun Samples; 30U cm^2 Area

magnitude below published values for Teflon. If one assumes that the published value of $10^{17}\Omega$-cm is accurate, then a parallel path having a resistance of about $4 \times 10^{11}\Omega$ is indicated by the data. This could be a surface leakage, or an edge leakage, or leakage through the sheath.

Values df $\delta_m = 3$ and $V_{max} = 300$ were used in the expression for Becondary emission, in accordance with the data giveh by Willis arld Skinner.[9] The values of C required ranged from 14.6 pf/cm2 at $V_B = 5$ kV to 10 pf/cm^2 at $V_B = 12$ kV and decreased monotonically with increasing beam voltage. Extrapolation of the curve to $V_B = 0$ indicates a dielectric constant for Teflon of -2.1. This decrease in effective capacitance is believed to be associated with edge effect#. Edge gradients are observed in the data. These become more pronounced at higher voltages reducing the effective area.[2] The value used fdr the backscatter coefficient varies about an order of magnitude for the Tehon samples. Not only does it change with beam voltage, but also appears to change during charging at a single beam voltage. Far the initial portio? of the charging curves, ξ varied from 0.25 at the lower beam voltages to 0.05 at high beam voltages. At equilibrium, ξ Varied from 0.02 at low beam voltages to 0.25 at high ones. These variatiohs were not linear; rather, τ was relatively constant at low and high beam voltages, with a transition occurring between $V_B = 8$ kV and $V_B = 12$ kV. Again, part of these variations may be due tb deviations of the actual secondary emission from-that calculated by the analytical expression being used.

Some investigation was undertaken to study the behavior of the Teflon samples duping arcing. Figure 4(a) shows a curve fit to a composite of two data sets for the initial chargin,; transient with a beam voltage of 16 kV. Figure 4(b) shows the

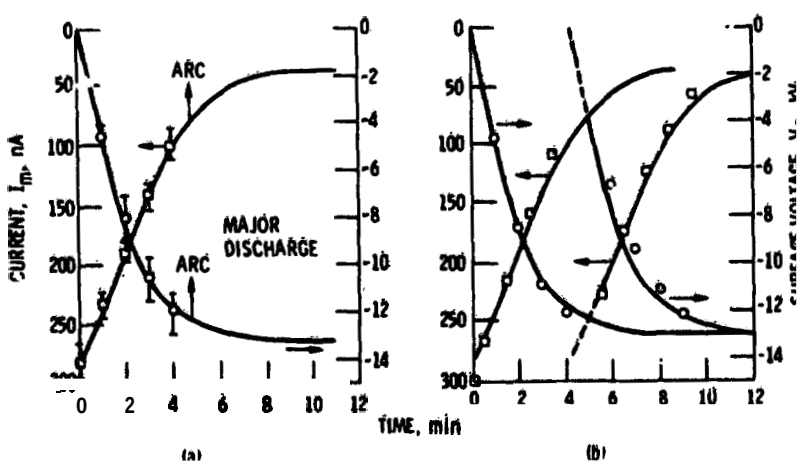

Figure 4. Comparison With Experimental Data, Discharge transients; silvered teflon samples; 16 kV beam

same calculated curves, this time with a single set of data. The left hand set of curves and points are the initial charging transient. An arc occurred on this sample between the time of the voltage reading at t = 4 min and that of the current reading taken at t = 5-1/2 min; the surface discharged, and charging was repeated. The curves shown for the post-arc charging transient are identical to those for the initial transient, but shifted in time. This indicates that the charging transient is quite repeatable, not only from test to test of Teflon samples, but also through arcing. That is, at least short term, the arcing does not affect the chargidg behavior of Teflon samples.

3.3 Composite Sample

One of the stated objectives of the present work was to investigate the "environment scaling" effects between the ground test and space environments. An obvious difference other than the environment between ground tests so far described and the space condition is that the studies of silvered Teflon discussed above were all conducted with the substrate grounded. In contrast. for the case of a spacecraft in orbit, the entire body, including the "grounds" must cdme into equilibriutn with the charged particle environment. The question of the behavior of a composite System becomes particularly interesting because of tne divergent time scales in which charging of "floating" metal plates and silvered Teflon above grbund are bbserved tb occur.

To investigate this question, a composite sample was built and tested. The sample consisted of an.electrically floating standard alumihum substrate with two strips of the 5 cm silvered tape mounted on it. This allowed for a 5 cm strip of the aluminum between the two Teflon strips to be etposed to the electron beam. The aluminum substrate was mounted in the test chamber in the same manner a6 the floating aluminum plate described in Section 3. 1. This configuration is depicted at the top of Figure 5(a). The bottom of this figure shows a vbltage trace at equilibrium for this sample.

The expectation was that this composite sample would charge in two stages because of the different effective capacitances through which the aluminum and the Teflon mult charge. The prediction, shown in Figure 5(b), is based on the idea that when the beam is turned on, the aluminum should charge to its equilibrium voltage with its time constant of seconds, carrying the Teflon voltage with it. When this has occurred, the Teflon should continue to charge froni tho equilibrium voltage of the aluminum to its own equilibrium voltage with its own time constant, that is, minutes. The curves in Figure 5(b) were thus obtained by superimposing the curves for aluminum above and for Teflon alone with the Teflon curve shifted so that it coincides with the aluminum curve at the point of equilibration for the aluminum. As can be seen from the data plotted in Figure 5(b), the expected behavior was found.

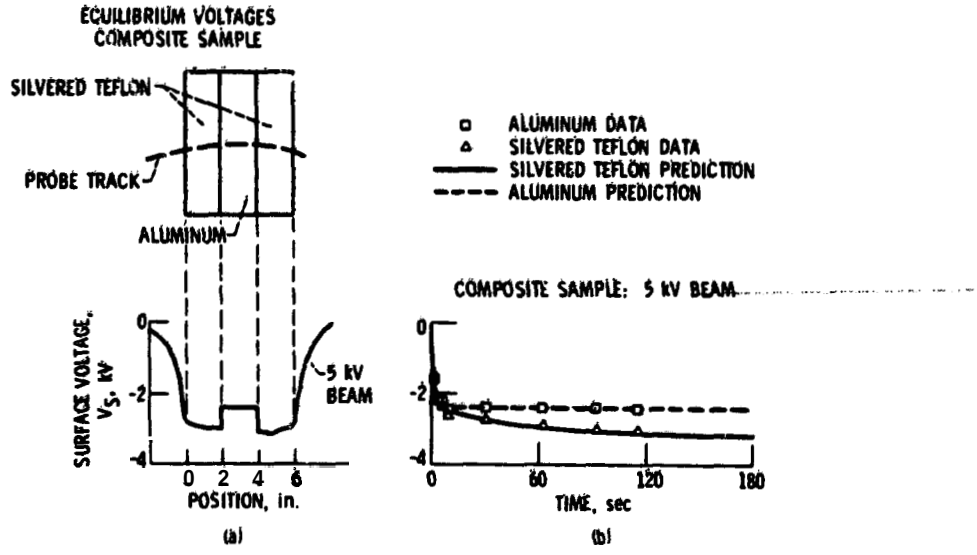

Figure 5. Silvered Teflon/Aluminum Composite Sample Floating

The expectation that the aluminum arid Teflon comprising the composite sample should charge to the same surface voltages as had the floating plate: and the Teflon samples above grounded substrates was based bn the observation that in both those cases the equilibration was dbmitiated by secahdary emission phenomena rather than by leakage currents tb ground. This is evidenced in two ways. First, plots of surface voltage at equilibrium versus beam voltage are straight lines; such behavior is supposed to be associated with emission dominated equilibration. Second, examination of printouts of the mbdel calculations reveals that, at equilibrium, the leakage current density term id several orders of magnitude smaller than the other currents in the mbdel. The conclusion, then, is that for this type of composite sample, each part responds to the charging environment with its characteristie time constant, and comes into equilibrium at its characteristic Burface voltage so long as leakage current does not play a dominant role in the equilibration.

It should be noted here that the tests run on this composite sample were not extensive. Further experimental investigation of this and other composite samples are planned.

1. ONE-DIMENSIONAL SPACE CHARGING MODEL

In order to predict charging behavior in space, a one-dimensional model for charging in space analogous to the one-dimendona1 ground test model was developed. The essential difference between the two models is that the space model assumes an isotropic Maxwellian particle distribution containing both electrons and ions and a Spherical collection geometry. The current densities ate derived from Langmuir probe calculations. This type of calculation has been used by several authors[4,5,6,10] to treat the spacecraft charging prablem. Derivation of the current density equations is given in Appendix B; a summary description is presented in Figure 6. As is indicated in this figure, the model as presented and ueed here assumes a geomagnetic substorm condition. That is, it assumes that V_s is negative, so that electrons are repelled and ions attracted. In these equations V_s is an algebraic quantity, that is, the sign id implicit.

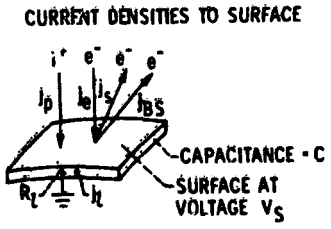

ASSUMPTIONS
GEOMAGNETIC SUBSTORM
ISOTROPIC MAXWELLIAN DISTRIBUTIONS
SPHERICAL COLLECTION GEOMETRY

CHARGING MODEL

$$-i_e(V_S) + i_p(V_S) + i_s(V_S) + i_{BS}(V_S) = i_t(V_S) + i_C(V_S,t)$$

FUNCTIONAL FORMS
DARK CONDITION – NO PHOTOEMISSION

SYMBOL & FORMULA	CURRENT DENSITY DUE TO
$i_e = i_{eo}\exp\left(\frac{V_S}{V_e}\right)$	PLASMA ELECTRONS
$i_p = i_{pO}\left(1 - \frac{V_S}{V_p}\right)$	PLASMA IONS
$i_s = i_{eo}\sqrt{\pi}\,7.4\,\delta_m \frac{V_e}{V_m}\,5i\left[i^5\mathrm{erfc}\left(\sqrt{\frac{V_e}{V_m}}\right)\right]\exp\left(\frac{V_e}{V_m} + \frac{V_S}{V_e}\right)$	SECONDARY ELECTRONS
$i_{BS} = \zeta i_{eo}\exp\left(\frac{V_S}{V_e}\right)$	BACKSCATTERED ELECTRONS
$i_t = \frac{V_S}{R_t} = \frac{V_S}{\rho t}$	LEAKAGE THROUGH INSULATOR
$i_C = C\frac{dV_S}{dt}$	SURFACE CHARGING

Figure 6. 1-D Model Space Substorm Environment

AB is evident from the sketch in Figure 6, secondary electrons due ta ion impact are not accounted fur in this model. This is because the intent here is to use material charging characteristics found by fitting the ground test model ta experimental data in conjunction with the space model to predict space charging. Since thefe were no ions used in the experiments, no coefficient for secondary electrons due to ion impact was determined. Therefore this current density source is riot considered. The surface voltage values predicted by this model are therefore somewhat largtr than. if secondary electrons due to ion impact had been included. For exarhple, a secondary coefficient of 1 would yield about a 10 percent reduction in the equilibrium voltage calculated for aluminum at V_e - 5 kV.

The procedure used to calculate charging is identical to that described for the ground test model. Material characteristics used were those determined by fitting the ground test model to the data. The capacitance of the aluminum (considered to represent the spacecraft "ground") was tak to be 15×10^{-11} farads, which is the capacitance of a one meter diameter sphere (to represent a "typical" spacecraft dimension) to infinity. This capacitance was chosen because the relevant capacitance f.·r charging flbating metal objects is that of the object to its surroundings. Those parameters (notably C and ξ for Teflon, and ξ far aluminum) which varied as functions of beam (and therefore surface) voltagr were associated with the equilibrium surface voltage for the appropriate test for purposes of making the space Voltage calculations. The relationships betweeh electron and ion temperatures and between temperatures arid current densities were taken from the Provisional Specification for the Geomagnetic Substorm Environment. ** This Specification is given as Figure 7. Thus, results of the space calculations, shown in Figure 8, ark given ad functions of electron temperature only

In Figure 8(b) two curves are shown for the surface voltage of silvered Tehon as a function of electron temperature. The first curve calculated used the experimentally determined value of 9×10^{15} Ω-cm for the effective resistivity of Teflon. This curve bends sharply to the right as electron temperature increases An inspection of the curreht densities driving tho equilibriutn indicated that leakage current played a large part in the equilibration of.the Teflon. Thus, this curve yiklda a "good" value for the surface voltage of Teflon if the spacecraft "ground" is actually near plasma ground. This would be the case if, for example, photoemission were holding the spacecr-ft ground near plasma ground and the Teflon surface of concern were shaded. However, if the spacecraft is assumed to be in eclipse. the aluminum representing the spacecraft ground is predicted to acquire a large negative voltage (solid line.). In this rase it is clear that leakage current can not drive the equilibration of the Teflon surface according to the dashed lint. Therefore a second curve was calculated for the Teflon, based on the assumption that there was no leakage. This is shown in the dash-dotted line.

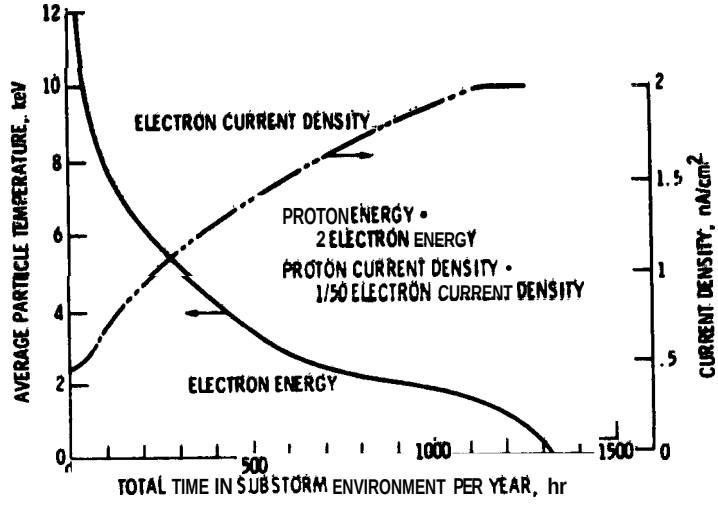

Figure 7. Provisional Specification for Satellite Time in a Geomagnetic Substorm Envirbnment (Ref. 11)

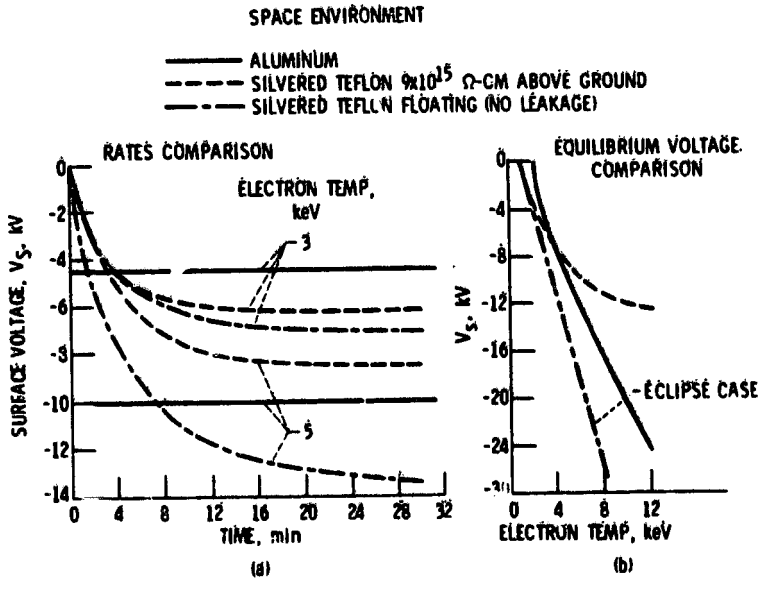

Figure 8. Fredictions of Charging Silvered Teflon and Aluminum Samples

Figure 8(a) shows the ratel of charging predicted for the space condition. The time to charge the aluminum is predicted to be seconds, comparable ta the time required tb charge the floating plate in the ground experiments. The time required to charge the Teflon is predicted tb be several minutes at lowel electron temperatures, ranging to tens of minutes as the electron temperature increases. Thus, equilibration of Teflon is predicted to require significantly longer time id space than it does in ground-experiments.

Using the curves shown in Figure 8, it is possible to predict the response of a "spacecraft", composed of an aluminum structure partially covered with silvered Teflod, to substorm and eclipse conditionb. Such a set of predictions is shbwn in Figure 9. For purposes of this figure, it is assumed that photoemission is sufficient to hold illuminated surfaces close to plasma ground.

Figure 9(a) assumes that the Teflon surface of interest is shaded when the spacecraft is in sunlight. A substorm injection with a 5 keV Maxwellian electron distribution is assumed to occur at t = 0 and this environment is assumed to remain constant throughout the time shown. An eclipse is assumed to occur ftom t = 60 min to t = 126 min. When the substorm occurs, the dark Teflon charges according to the dashed curve of Figure 8(a), shown in Figure 9 as a solid curve; the aluminum at "ground" is assumed to be Held near plasma ground by photoemission. ...The Teflon surface reaches its leakage dominated equilibrium voltage

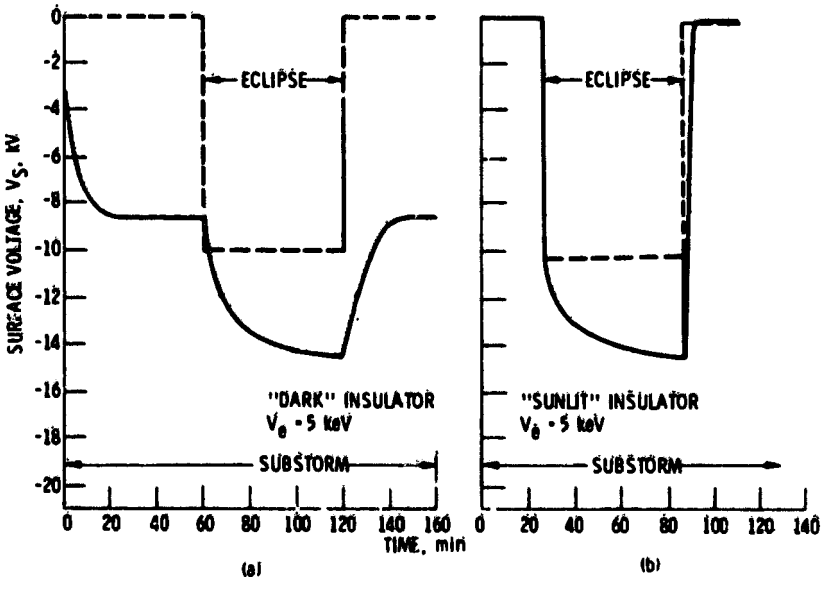

Figure 9. Reeponse to Substorm and Eclipse. 1-D Model Predictions

of -8.5 kV with its time constant of about 20 min. When the spacecraft enters eclipse, the aluminum charges quickly (in seconds) to its equilibrium voltage of -10 kV. It is assumed that the charge on the Teflon surface is immobile on this time scale, so this surface remains at -8.5 kV. At this point, the leakage current, which was driven by the voltage differential of 8.5 kV disappears, so the Teflon finds itself to be no longer in equilibrium with its environment and proceeds to charge to its "floating" value of ~-14.5 kV in a characteristic 20-30 mid period. Upon exit from eclipse, a similar pattern is followed. The aluminum falls quickly to near plasma ground. Because this discharging is driven by photoemission, it requires only about 0.02 sec for the aluminum to reach plasma ground (assuming $\sim 10^{-9}$ A/cm^2 photocurrent). Now, the Teflon again finds itself out of equilibrium with its plasma environment, and proceeds to discharge slowly to its previous equilibrium potential of -8.5 kV.

Figure 9(b) shows a similar type of time history for an insulating surface which is exposed to sunlight. Again, the solid line represents the surface voltage of the Teflon and the dashed line the spacecraft ground. The entry into eclipse and subsequent charging up is analogous to the charging of the composite sample discussed in Section 4. The aluminum charges rapidly (in seconds) to its equilibrium value. Because the Teflon had no significant charge on its surface, its voltage follows that of the aluminum until the aluminum reaches equilibrium. The Teflon then continues to charge slowly to its equilibrium potential. Upon exit from eclipse, both the aluminum and the Teflon are discharged by photoemission. Thus, the aluminum reaches plasma ground in about 0.02 sec, as in the previous case. The Teflon also discharges more quickly than it charged; it requires about 4 min to reach plasma ground.

These results indicate a need for charging studies which take into account relative charging rates as well as different equilibrium charging levels of various spacecraft surfaces. A "typical" spacecraft has several different types of surfaces (solar cells, thermal blankets, etc.) each of which can be expected to charge with its own time constant. The importance of the effect of the different time constants should be assessed.

5. CONCLUDING REMARKS

The present study has resulted in the development of a set of "material charging characteristics" which describe the charging of small (300 cm^2) samples of 5 mil silvered Teflon and oxidized aluminum. Based on these characteristics, predictions of charging in space have been made and used to estimate the behavior of a composite body under conditions of substorm and eclipse. Several interesting

differences between charging behavior under ground test conditions and predicted behavior in space have been noted for silvered Teflon. Under ground test conditions silvered Teflon acquires the same surface potential mounted on grounded and floating substrates because the equilibration is dominated by surface emission phenomena. However, in space, significant differences are predicted in surface voltage for these two mounting configurations. This is because leakage current dominates the equilibration of the Teflon When the aluminum is at ground, while surface emission dominates for the floating aluminum case. The time required for silvered Teflon to charge to equilibrium in tests is several minutes; this time is predicted to be several tens of minutes in space.

In contrast to the several minutes to several tens of minutes time scales for silvered Teflon, floating aluminum samples are observed in ground test and predicted in space to charge to equilibrium in seconds Their capacitance is much lower than that of Teflon since it is determined by their surroundings. There are also orders of magnitude differences in time scales far discharging by photoemission of aluminum and Teflon. This discrepancy in charging and discharging rates gives rise to sudden changes in the electric fields which the Teflon must sustain upon entry into and exit from eclipse. It is felt that these differential charging rates as well as differential charging levels may be important and should be investigated further. Thus, transient (quasistatic) as well as steady stare models should be developed for charging.

The one-dimensional models described herein have been found useful in the interpretation of experimental results. and as guides to relating test results to expected space behavior. Models of ground test situations are needed since they can be used interactively with test data. This is especially true since it is impossible, or at least impractical, to simulate accurately the geosynchronous environment. Thus environment scaling must be done through use of models, at least for the present.

Finally, higher dimensional models are needed One-dimensional models ran not account for such things as edge effectsor interactions between adjacent surfaces at differeht potentials as with different charging properties Such effects are clearly important.[2] and may dominate the charging behavior of multisurface samples and spacecraft.

References

1. Berkopec, F. D., Stevens, N. J., and Sturman, J. C. (1976) The LeRC substorm simulation facility, Paper III-1, Spacecraft Charging Technology Conference, Colorado Springs, Colo.
2. Stevens, N. J., Berkopec, F. D., Staskus, J. V., and Bloch, R. A. (1976) Testing of typical spacecraft materials in a simulated substorm environment, Paper III-2, Spacecraft Charging Technology Conference, Colorado Springs, Colo.
3. DeForest, S. E. (1972) Spacecraft charging at synchronous orbit, J. Geophys. Res. 77:651.
4. Fredericks, R. W., and Scarf, F. L. (1973) Observations of spacecraft charging effects in energetic plasma regions, in Photon and Particle Interactions with Surfaces in space, R. J. L. Grard, Editor, D. Reidel Publ. Co., Dordrecht, Holland.
5. Inouye, G. T. (1975) Spacecraft charging model, AIAA paper 75-255, AIAA 13th Aerospace Sciences Meeting, Pasadena, California
6. Roseh, A. (1975) Spacecraft charging: Environment induced anomalies, AIAA Papel' 79-91, AIAA 13th Aerospace Sciences Meeting, Pasadena, California.
7. Gibbons, D. J. (1966) Secondary electron emission, in Handbook of Vacuum Physics, Vol 2, A. H. Beck. Editor. Pergamon Press, Oxford, England
8. Sternglass, E. J. (1950) J. Phys. Rev. 80:925
9. Willis, R. F., and Skinner, D. K. (1973) Secondary electron remission yield behavior of polymers, Solid State Communications 13:1485
10. Cauffman, D. P. (1975) Inclusion of secondary electrons in models of equilibrium potentials, Paper SA63 Presented et the Spring AGU Meeting, Washington, D. C.
11. Lovell., R. R., Stevens, N. J., and Purvis, C. K. (1976) Provisional specification for satellite time in a geomagnetic substorm environment, Paper V-2, Spacecraft Charging Technology Conference, Colorado Springs, Colo.
12. Langmuir, I., and Matt-Smith, H. ill. (1926) The theory of collectors in gaseous discharges, Phya. Rev. 28 (No. 4):717.
13. Grard, R. J. L., Knott, K., and Pederson, A. (1973) The influence of photo. electron and secondary electron emission oh electric field measurements in the magnetosphere and solar wind, in Photon and Particle Interaction with Surfaces in Space, R. J. L. Grard, Editor, D. Reidel, Dordrecht, Holland.
14. Abramowitcz, M., and Stegun, I. A., Editors (1968) Handbook of Mathematical Functions, Dover Publications, Inc., New York.

Appendix A

One-Dimensional Ground Test Model

In this model, electrons from the electron gun are assumed to approach the planar sample normally. All motion is restricted to the x direction (see Figure A1). The electron beam is assumed monoenergetic, with energy

$$E_B \triangleq e V_B$$

where e is the electronic charge and V_B the beam voltage. The current density emitted from the gun is given by

$$j_o = n_o e \left(\frac{2E_B}{m_e}\right)^{1/2} \tag{A1}$$

where n_o = particle density. It is assumed here that $n_o e$ (the charge density) is constant, in order to account for the spreading of the beam in the real situation. Thus the continuity equation requires that some particles are "lost".

We wish to calculate current densities to the sample surface. Current densities to be considered are those due to primary electrons, secondary electrons, backscattered electrons, and leakage through the bulk of the insulator. The insulator is assumed to be mounted above a grounded substrate for purposes of calculating leakage.

Throughout this development the sample surface is assumed negative, and all secondary and backscattered electrons are assumed to escape. All signs are given explicitly so that symbols represent positive quantities.

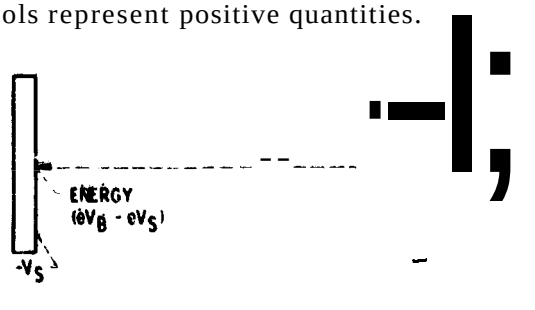

Figure A 1.

2. CURRENT DENSITY DUE TO PRIMARY ELECTRONS

Consider electrons approaching the sample with energy E. It is assumed that the electrons do not collide with one another, and that motion is restricted to one-dimension. If the sample surface has a repulsive potential of magnitude V_S, energy conservation requires that they arrive at the surface with energy $E-eV_S$. Since all electrons leave the gun with energy eV_B, the current density to the sample surface is simply

$$j_e = n_o e \left(\frac{2}{m_e}\right)^{1/2} (eV_B - eV_S)^{1/2} \tag{A2}$$

Rearranging and using Eq. (A1), we find

$$j_e = j_o \left(1 - \frac{V_S}{V_B}\right)^{1/2} \tag{A3}$$

since we are requiring that $n_o e$ remain constant.

3. CURRENT DENSITY DUE TO SECONDARY ELECTRONS

Sternglass[1] has given the following expression for secondary yield as a function of primary electron energy at impact:

$$\delta(E_i) = 7.4\,\delta_m \frac{E_i}{eV_m} \exp\left[-2\left(\frac{E_i}{eV_m}\right)^{1/2}\right] \tag{A4}$$

where δ_m is the maximum yield, eV_m is the primary energy for which maximum yield is attained and E_i is primary energy at impact From the discussion given in Eq. (A2) above, for this rase

$$E_i = eV_B - eV_S \tag{A5}$$

The secondary current dedsity *is* then

$$j_s = j_e\,\delta(eV_B - eV_S) \tag{A6}$$

which is

$$j_s = j_o\, 7.4\, \delta_m \frac{V_B}{V_m} \left(1 - \frac{V_S}{V_B}\right)^{3/2} \exp\left[-2\left(\frac{V_B - V_S}{V_m}\right)^{1/2}\right]. \qquad (A7)$$

4. CURRENT DENSITY DUE TO BACKSCATTERED ELECTRONS

No analytical expression was found for backscattered electron emission. For simplicity, it was therefore assumed that backscattered electron current density represents a fraction of the incident current density. Thus,

$$j_{BS} = \xi j_e = \xi j_o \left(1 - \frac{V_S}{V_B}\right)^{1/2} \qquad (A8)$$

5. LEAKAGE CURRENT DENSITY

Leakage current is generally represented by

$$i_l = \frac{V_S}{R} \qquad (A9)$$

In terms of bulk resistivity this is

$$i_l = \frac{V_S A}{\rho \ell} \qquad (A10)$$

Where ρ is bulk resistivity, A is the area and the thickness of the Bample. Then

$$j_l = \frac{i_l}{A} = \frac{V_S}{\rho \ell} \qquad (A11)$$

6. THE 1-D MODEL

The primary electron current density represents a source of electrbns arriving at the sample. The other three current densities repredent loss of electrons froni the surfaee. Thus the net current density to the eurface is

$$j_c = j_e - j_s - j_{BS} - j_l \tag{A 12}$$

This net current density plays the role of a charging current to the surface. Thus, if we represent the sample's charging as the charging of a capacitor, we have

$$j_c = C \frac{dV_S}{dt} = j_e - j_s - j_{BS} - j_e \tag{A 13}$$

where C is capacitance, here expressed in farads per square centimeter to main; tain consistency of units. Equation (A 13) is solved id the manner described in the test on a computer to calculate the charging.

It remains t6 associate the experimentally measured parameters, Surface vbltage, and total current tb ground, with calculated values. The surface voltage association is trivial; it is simply $-V_S$. The tbtal current tb ground is the charging current plus the leakage current for the eample as a whole. Thus

$$I_M = A(j_c + j_l) \tag{A 14}$$

References

1. Sternglass, E. J., (1950) J. Phys. Rev. 80:925.

Appendix B

One-Dimensional Space Substorm Model

I. INTRODUCTION

The one-dimensional space model assumes a two-dimensional isotropic Maxwellian Velocity distribution for primary particles, add a spherical collection geometry. The calculation$ are essentially those for a spherical Langmuir probe. The present calculations are based on the work of Langmuir[1] and Grard et al,[2] and follow clobely the derivation of Cauffman.[3] The latter work has not been published; therefore portibns of it are reproduced here for clarity. Such portions are identified by superscript reference.

Geometry for the calculations is depicted in Figure B1.[3] The sheath is assumed *to* have radius a, and the collectbr radius R. The radial and tangential velocity components in the "undisturbed" region (sheath edge) are v_r and v_t, respectively, and those at the collector Burface u_r and u_t. The surtace potential of the collector is V_S. The potential in the sheath is assumed to be a function of radial distance from the collector and to be monotonic. The plasma is assumed collisionless, that is, orbit limited theory applies, and energy and angular momentum ark assumed constaht for each particle.

The integral requiring solution fbr current densities due to primary electrons[3,2] and ions, and backscattered electrons is

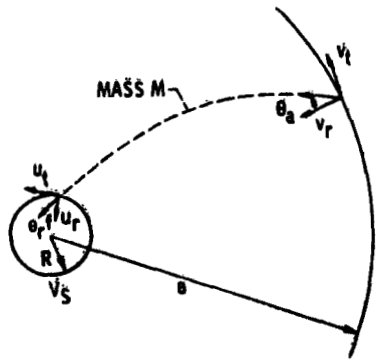

Figure B1.

$$j_i = \frac{i_i}{4\pi R^2} = \frac{4\pi a^2}{4\pi R^2} \int_0^{\pi/2} d\theta_R \int_0^{\infty} dE_R \frac{dj_i}{dE_R}(E_r, \theta_R) \qquad (B1)$$

where the subscript i stands for either e (electrons) or p (H+ ions), and θ_R and E_r are the angle and energy at impact on the collector (see Figure B1).

For secondary electron current, solution must be found for[3.2]

$$j_S = \frac{i_e}{4\pi R^2} = \frac{4\pi a^2}{4\pi R^2} \int_0^{\pi/2} d\theta_R \int_0^{\infty} dE_R \frac{dj_R}{dE_R}(E_R, \theta_R)\, \delta(E_R) \qquad (B2)$$

where $\delta(E_R)$ is the secondary electron yield as a function of electron impact energy.

These integrations cannot be performed directly because the distribution function for the particles at the collector is unknown, and therefore we can not determine dj_i/dE_R. However, we do know the distribution at the sheath edge, and can therefore determine dj_i/dE_a. If we assume the plasma to be collisionless, we can also convert the limits on E_R and θ_R to limits on E_a and θ_a, and perform the required integrations bn these variables.

1.1 Conditions for Collection

In order to contribute to current collected at R, a particle must have energy $E_R \geq 0$ and direction $0_R \leq \theta \leq \pi/2$. Since the plasma is assumed collisionless and V(r) is assumed monatonic, each particle's energy and angular momentum must be conserved. Assume the particles of interest have charge -e. Energy conservation demands

$$\frac{1}{2} m_i (u_r^2 + u_t^2) = \frac{1}{2} m_i (v_r^2 + v_t^2) + eV_S \quad (\rightleftharpoons) \quad E_R = E_a + eVS \qquad (B3)$$

Angular momentum conservation demands

$$Ru_t = av_t \quad (\rightleftharpoons) \quad Ru \sin\theta_R = av \sin\theta_a \qquad (B4)$$

where

$$u = (u_r^2 + u_t^2)^{1/2} \quad \text{and} \quad v = (v_r^2 + v_t^2)^{1/2}$$

Solving for E_a and θ_a in terms of E_R and θ_R yields the conditions for collection3

$$0 \le \theta_R \le \frac{\pi}{2} \Longrightarrow 0 \le \theta_a \le \sin^{-1}\left[\frac{R}{a}\left(\frac{E_a + eV_S}{E_a}\right)^{1/2}\right] \triangleq \theta_o$$

$$\infty > E_R \ge 0 \Longrightarrow \infty > E_a \ge E_o \triangleq \begin{cases} 0 \quad \text{for } V_S > 0 \text{ (attraction)} \\ -eV_S \text{ for } V_S \le 0 \text{ (repulsion)} \end{cases} \tag{B5}$$

1.2 Energy Format

An isotropic Maxwellian velocity distribution in three-dimensions has a distribution given by

$$f(\vec{v}) = \left(\frac{m_i}{2\pi eV_i}\right)^{3/2} \exp\left[\frac{-m_i\vec{v}\cdot\vec{v}}{2eV_i}\right] . \tag{B6}$$

We are interested in a two-dimensional distribution which can be fouhd from

$$g(v_r, v_t) = \int_0^{2\pi} f(v_r, v_t \sin\chi, v_t \cos\chi)\, d\chi \tag{B7}$$

Substituting for $f(\vec{v})$ and integrating, we have

$$g(v_r, v_t) = \frac{1}{\sqrt{2\pi}}\left(\frac{m_i}{eV_i}\right)^{3/2} v_t \exp\left[\frac{-m_i(v_r^2 + v_t^2)}{2eV_i}\right] . \tag{B8}$$

Langmuir1 gives the incremental current across the sheath as

$$d_i = 4\pi a^2 n e v_r g(v_r, v_t)\, dv_r\, dv_t . \tag{B9}$$

Then,

$$dj_i = \frac{di_i}{4\pi R^2} = \frac{a^2}{R^2}\frac{n_i e}{\sqrt{2\pi}}\left(\frac{m_i}{eV_i}\right)^{3/2} v_r v_t \exp\left[\frac{-m_i(v_r^2 + v_t^2)}{2eV_i}\right] dv_r\, dv_t \tag{B10}$$

arid, changing to E_a, θ_a coordinates we Have3

$$dj_i = \frac{a^2}{r^2} n_i e \left(\frac{eV_i}{2\pi m_i}\right)^{1/2} \frac{2}{(eV_i)^2} E_a \exp\left[-\frac{E_a}{eV_i}\right] \sin\theta_a \cos\theta_a d\theta_a dE_a \qquad (B11)$$

as required.

2. PRIMARY AND BACKSCATTERED PARTICLE CURRENT DENSITIES

Since backecattered electrorl current density is considered to be simply a fraction of the incident electron current density, the Same integration applies tb both. The calculation for positive ion collectibn is the same as for electron collection with apprapriate sign changes to account for the positive charge, and using the ion mass and temperature. In Eqs. (B9) to (B11), the sign on the leading charge has been Suppressed. Appropriate sighs will be supplied id Section B. 5.

The integration to be performed is

$$j_i = \frac{a^2}{R^2} n_i e \left(\frac{eV_i}{2\pi m_i}\right)^{1/2} \frac{2}{(eV_i)^2} \int_{E_0}^{\infty} \int_{0}^{\theta_0} \sin\theta_a \cos\theta_a E_a \exp\left(-\frac{E_a}{eV_i}\right) d\theta_a dE_a. \qquad (B12)$$

Cauffman3 evaluates this integral and finds, in agreement with Langmuir 1

$$j_i = j_{io} \exp\left(\frac{V_S}{V_i}\right) \qquad V_S \leq 0 \text{ (Repulsive)}$$

$$j_i = j_{io}\left(1 + \frac{V_S}{V_i}\right) \qquad V_S \geq 0 \text{ (Attractive)} \qquad (B13)$$

where

$$j_{io} = n_i e \left(\frac{eV_i}{2\pi m_i}\right)^{1/2}$$

Since the interest here is in modeling charging in substorms with no photoemission, we expect V_S negative. Thus, electrons are repelled and ions attracted. So we have for electrons

$$j_e = j_{eo} \exp\left(\frac{V_S}{V_e}\right) \qquad (B14)$$

for ions

$$j_p = j_{po}\left(1 - \frac{V_S}{V_p}\right) \tag{B15}$$

where the minus sign reflects the fact that ions are attracted by negative V_S. For backecattered electrons,

$$j_{BS} = \xi j_e = \xi j_{eo} \exp\left(\frac{V_S}{V_e}\right) \tag{B16}$$

where ξ is the backscatter coefficient.

3. SECONDARY ELECTRONS DUE TO ELECTRON IMPACT

Secbndary yield as a function of electron impact energy has been given by Sternglass[4] as

$$\delta(E_R) = 7.4\,\delta_m \frac{E_R}{eV_m} \exp\left[-2\left(\frac{E_R}{eV_m}\right)^{1/2}\right] \tag{A4}$$

where δ_m is the maximum yield and eV_m the energy at which the maximum yield is obtained. To determine secondary electron current density, we must multiply the left hand Bide of equatian (B11) by $\delta(E_R)$ and integrate. Thus we need

$$j_s = \frac{a^2}{R^2} \cdot o \frac{2}{(eV_e)^2} \frac{7.4\,\delta_m}{eV_m} \int_{E_0}^{\infty} \int_{0}^{\theta_0} E_a (E_a + eV_S)$$

$$\times \exp\left[\frac{-E_a}{eV_e} - 2\left(\frac{(E_a + eV_S)}{eV_m}\right)^{1/2}\right] \sin\theta_a \cos\theta_a \, d\theta_a \, dE_a \tag{B17}$$

which is Cauffman's[3] equatibn for secondary electrons, except that he uses a $\sec\theta_r$ dependence of ξ on θ_r whlch is not used here. The θ_a integral is the Bame as before and yields

$$j_s = j_{eo} \frac{7.4\,\delta_m}{(eV_e)^2 eV_m} \int_{E_0}^{\infty} (E_a + eV_S)^2 \exp\left[\frac{-E_a}{eV_e} - 2\left(\frac{E_a + eV_S}{eV_m}\right)^{1/2}\right] dE_a \tag{B18}$$

Now, sequentially setting $\chi^2 = E_a + eV_S$ and $\eta = (eV_e)^{-1/2}\,\chi + \left(\frac{V_e}{V_m}\right)^{1/2}$ and substituting, we find

$$j_S = 2j_{eo}\,7.46_m\,\frac{V_e}{V_m}\exp\left(\frac{V_S}{V_e}+\frac{V_e}{V_m}\right)\int_{\eta_o}^{\infty}\left[z-\left(\frac{V_e}{V_m}\right)^{1/2}\right]^{\delta}\exp(-\eta^2)\,d\eta \qquad \text{(B19)}$$

where

$$\eta_o = \begin{cases}\left(\frac{V_S}{V_e}\right)^{1/2}+\left(\frac{V_e}{V_m}\right)^{1/2} & \text{for } V_S > 0\\ \left(\frac{V_e}{V_m}\right)^{1/2} & \text{for } V_S \le 0\end{cases}$$

Since we are considering substorm cases only here, the condition $V_S \le 0$ is of interest. For this case the integral in Eq. (B19) is just

$$J = \int_{\left(\frac{V_e}{V_m}\right)^{1/2}}^{\infty}\left[\eta-\left(\frac{V_S}{V_m}\right)^{1/2}\right]^{5}\exp(-\eta^2)\,d\eta\,. \qquad \text{(B20)}$$

Recalling the expression for repeated integrals of the errur function complement[5]

$$i^n\,\mathrm{erfc}(z) = \frac{2}{\sqrt{\pi}}\int_z^{\infty}\frac{(t-z)^n}{n!}\exp(-t^2)\,dt \qquad \text{(B21)}$$

where, by definition,

$$i^n\,\mathrm{erfc}(z) = \int_e^{\infty} i^{n-1}\,\mathrm{erfc}(t)\,dt$$

and

$$i^0\,\mathrm{erfc}(z) = \frac{2}{\sqrt{\pi}}\int_z^{\infty}\exp(-t^2)\,dt = \mathrm{erfc}(z)$$

and identifying t, z and n with the appropriate variables In (B20), we have

$$\mathcal{I} = \frac{\sqrt{\pi}}{2} 5! \; t^5 \operatorname{erfc}\left(\sqrt{\frac{V_e}{V_m}}\right). \tag{B22}$$

So, from Eqs. (B19) and (B22), we have

$$j_S = \sqrt{\pi}\; j_{eo}\, 7.46_m \frac{V_e}{V_m} 5! \left[t^5 \operatorname{erfc}\left(\sqrt{\frac{V_2}{V_m}}\right)\right] \exp\left(\frac{V_S}{V_e} + \frac{V_e}{V_m}\right) \tag{B23}$$

and we note that the dependence of j_s on V_S is the Same as that of j, and j_{BS}.

1 .LEAKAGE CURRENT DENSITY

Leakage current density is defined in the same manner for the space model as it was for the test facility model (see Section 5 of Appendix A). Thus, we have

$$j_1 = \frac{V_S}{\rho p}$$

where ρ is bulk resistivity and 1 is the thickness of the insulating film.

5. THE 1-D SPACE MODEL

Now, the net current density to the sample surface is

$$j_c = -j_e + j_p + j_s + j_{BS} - j_1 \tag{B25}$$

where the signs on the current densities are given explicity here, and we recall that V_S in thts model is algebraic (that is, can be positive or negative), although the derivations have assumed it negative.

The net current density plays the role of a charging current to the surface, so that

$$j_c = C \frac{dV_S}{dt} = -j_e + j_p + j_s + j_{BS} - j_1 \tag{B26}$$

where C is capacity expressed in farads per square centimeter and where we assume we are chargi .g a capacttor. Equation (B26) is solved in the same wny as Eq. (A13) on a computer to determine V_S versus ttmc for charging,

Referentes

1. Langmuir, I., and Mott-Smith, H. M. (1926) The theory of collectors in gaseous discharges, Phys. Rev. 28(No. 4):717.
2. Grard, R. J. L., Knott, K., and Pederson, A. (1973) The influence of photo-electron arid secondary electron emission on electric field measurements id the magnetosphere and solar wind, in Photon and Particle Interaction with Surfaces in Space, R. J. L. Crard, Editor, D. Reidel, Dordrecht, Wolladd.
3. Cauffman, D. P. (1975) Inclusion of secondary electrons in models of equilibrium pbtentials, Paper SA63 Presented at the Spring AGU Meeting, Washington, D. C.
4. Sternglass, E. J., (1950) J. Phys. Rev. 80:925.
5. Abramowitcz, M., and Stegun, I. A., Editors (1968) Handbook of Mathematical Functions, Dover Publications, fnc., New York.